

N-Heterocyclic carbenes derived from imidazo[1,5-*a*]pyridines related to natural products: synthesis, structure and potential biological activity of some corresponding gold(I) and silver(I) complexes

Monica Mihorianu^a, M Heiko Franz^{b,c}, Peter G Jones^a, Matthias Freytag^a, Gerhard Kelter^d, Heinz-Herbert Fiebig^d, Matthias Tamm^{a*} and Ion Neda^{a,c,*}



A series of Au(I) complexes (12–16) and Ag(I) complexes (17–20) derived from imidazo[1,5-*a*]pyridin-3-ylidenes were synthesized from AuCl(SMe₂) or by reacting silver(I) acetate with 2,5-dimethylimidazo[1,5-*a*]pyridin-2-ium iodide or imidazo[1,5-*a*]pyridin-2-ium salts, and were characterized using NMR spectroscopy, mass spectrometry and elemental analyses. In addition, the Au(I) complex 13 and the Ag(I) complex 19 were characterized using single-crystal X-ray diffraction. Using paclitaxel as a standard, all Au(I) and Ag(I) N-heterocyclic carbene complexes were evaluated for their *in vitro* anti-tumour activity against 12 cell lines using a monolayer cell survival and proliferation assay. The highest anticancer activity was found for complexes 15, 13 and 14 with mean IC₅₀ values of 10.09, 10.42 and 12.28 μM, respectively. Copyright © 2016 John Wiley & Sons, Ltd.

Additional supporting information may be found in the online version of this article at the publisher's web site.

Keywords: Ag(I) N-heterocyclic carbene complexes; Au(I) N-heterocyclic carbene complexes; anti-tumour agents; imidazo[1,5-*a*]pyridin-3-ylidenes

Introduction

Imidazo[1,5-*a*]pyridines are an important class of heterocyclic compounds because of their unique biological^[1–4] and photophysical properties leading to potential applications in organic light-emitting diodes^[5] and in organic thin-layer field-effect transistors.^[6] Recently, they have also been used as precursors of N-heterocyclic carbenes (NHCs)^[7,8] whose synthesis and applications are still under investigation.

Imidazo[1,5-*a*]pyridine NHC derivatives are interesting ligands in homogeneous catalysis^[9] and exhibit promising biological properties.^[10] Furthermore, their ability to form stable metal complexes and their facile derivatization make them suitable candidates for drug development. In addition, the imidazo[1,5-*a*]pyridine core represents an important part of the cribrostatin-6 (I) skeleton (Fig. 1). Compound I was isolated from the sea sponge *Cribochalina*. It possesses anticancer activity, and antibacterial and antifungal properties, inhibiting growth in a variety of pathogens.^[11]

The discovery of platinum-based anti-tumour agents^[12] (e.g. cisplatin,^[13] carboplatin and oxaliplatin) opened a new chapter in medicine – metal-containing complexes with anticancer activity. Over time, other transition metals such as rhodium, palladium, silver and gold have, at least in part, replaced platinum, in order to reduce severe (toxic) effects associated with platinum anticancer complexes.^[14] For example, auranofin,^[15] a monomeric gold(I) phosphine drug, was introduced and approved by the US Food and Drug Administration for the treatment of rheumatoid arthritis in 1985. Nowadays, Aurothiomalate, Aurothioglucose and

Auranofin are registered trademarks. However, resistance phenomena complicate the clinical applications of anticancer drugs. To overcome this problem, it is necessary to create new cytotoxic complexes by metal variation and development of new carrier ligands. These ligands should be easily accessible in a few reaction steps and allow for a wide variation of their substitution pattern in order to tune their reactivity in biological media. NHCs fulfil all these requirements and permit the design and synthesis of cytotoxic and antibacterial transition metal complexes.^[16,17]

Among the non-platinum drugs, silver(I)^[18] and gold(I) NHC complexes^[19] have attracted the most attention. Recent studies have shown that silver(I) NHC complexes display *in vitro* anticancer activity against ovarian and breast cancer cells,^[20] whereas gold(I)

* Correspondence to: Matthias Tamm or Ion Neda, Institut für Anorganische und Analytische Chemie, Technische Universität Carola Wilhelmina, Hagenring 30, D-38106 Braunschweig, Germany. E-mail: m.tamm@tu-bs.de

† Dedicated to Henning Hopf on the occasion of his 75th birthday

a Institut für Anorganische und Analytische Chemie, Technische Universität Carola Wilhelmina, Hagenring 30, D-38106, Braunschweig, Germany

b InnoChemTech GmbH, Hagenring 30, D-38106, Braunschweig, Germany

c Institutul National de Cercetare Dezvoltare pentru Electrochimie si Materie Condensata, Str. Dr A. Paunescu Podeanu Nr 144, Ro-300569, Timisoara, Romania

d Oncotest GmbH, Am Flughafen 12-14, D-79108, Freiburg, Germany

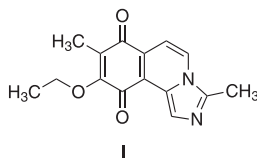


Figure 1. Structure of 9-ethoxy-3,8-dimethylimidazo[5,1-*a*]isoquinoline-7,10-dione (cribrostatin-6) (I).

NHC complexes inhibit the enzyme thioredoxin reductase,^[21] which promotes the proliferation of tumour tissue and whose inhibition is related to the triggering of anti-mitochondrial effects. These results have encouraged further medicinal applications of NHC complexes of gold(I) and silver(I).^[22]

We are interested in the imidazo[1,5-*a*]pyridine moiety as a scaffold for new anticancer drugs, since it is readily accessible^[23] and since its derivatives have proved to be valuable antimicrobial agents.^[24] Furthermore, imidazo[1,5-*a*]pyridines of type **II** (Fig. 2) can be easily modified by N-alkylation, and the resulting imidazo[1,5-*a*]pyridin-2-ium salts (**III**) may serve as precursors for the preparation of very stable transition metal complexes with NHCs of the imidazo[1,5-*a*]pyridin-3-ylidene type (**IV**).^[7–10]

Herein, we report the preparation, characterization and biological studies of two new series of unsymmetrically substituted NHC gold(I) and silver(I) complexes derived from imidazo[1,5-*a*]pyridines. The design and synthesis of NHC–gold(I) chloride complexes were inspired by recent work on benzimidazol-2-ylidene gold(I) complexes.^[25] Gold(I) was selected rather than gold(III) because it is more thermodynamically stable, less oxidizing and less toxic. Furthermore, based on recent anticancer and antimicrobial studies of NHC–silver(I) acetate complexes^[26] and the pressing interest in finding new silver-based antimicrobials active against resistant organisms, we chose to synthesize and investigate a series of imidazo[1,5-*a*]pyridine-3-ylidene silver(I) acetate complexes.

Experimental

General Comments

Chemicals and solvents were obtained from commercial sources, and all reagents were of analytical grade and used as received without further purifications. NMR spectra were recorded at room temperature with a Bruker AV II-300 at 300 MHz for ¹H NMR and 75 MHz for ¹³C NMR or an AV III-600 spectrometer. ¹H NMR and ¹³C NMR peaks are labelled as singlet (s), doublet (d), triplet (t), quartet (q), doublet of doublets (dd), doublet of doublets of doublets (ddd), doublet of doublets of doublets of doublets (dddd), multiplet (m). Chemical shifts (δ) were measured relative to tetramethylsilane peak set at 0.00 ppm. The imidazo[1,5-*a*]pyridine core is labelled according to the rules of IUPAC. Examples of the numbering are given in the supporting information. ESI-MS spectra were measured with a Finnigan LC Q Deca spectrometer using MeOH or AcCN as carrier solvent. EI-MS spectra were measured with a Finnigan MAT 8400-MSS and Finnigan MAT 4515 spectrometer. All reactions

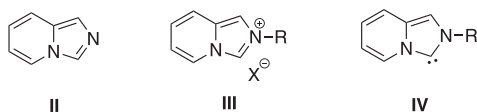


Figure 2. Schematic representations of imidazo[1,5-*a*]pyridine (**II**), imidazo[1,5-*a*]pyridin-2-ium salts (**III**) and their corresponding NHC derivatives (**IV**).

were carried out under inert atmosphere and in the absence of light where applicable.

General Procedure for Synthesis of Imidazo[1,5-*a*]pyridin-2-ium Salts (7–11)

Imidazo[1,5-*a*]pyridines **2** and **6** (1 equiv.) were dissolved in tetrahydrofuran (THF), treated with stirring with the respective alkyl halides (5 equiv.) and heated at 60 °C for 3–10 h. The resulting suspension was cooled and filtered to afford the pure products as solids.

2-Methylimidazo[1,5-*a*]pyridin-2-ium iodide (7) (C₈H₉N₂I). Starting materials: methyl iodide (1.2 g, 8.46 mmol) and imidazo[1,5-*a*]pyridine (**2**; 0.2 g, 1.69 mmol). Yield 0.36 g (1.38 mmol, 82%); yellow hygroscopic solid. ¹H NMR (300 MHz, DMSO-*d*₆, δ , ppm): 9.68 (s, 1H, H3), 8.62 (dd, *J* = 6.9, 1.2 Hz, 1H, H5), 8.20 (s, 1H, H1), 7.94–7.80 (m, 1H, H8), 7.37–7.10 (m, 2H, overlapping signals for H6, H7), 4.19 (s, 3H, N2 CH₃). ¹³C NMR (75 MHz, DMSO-*d*₆, δ , ppm): 129.05 (CH, C3), 126.88 (CH, C5), 124.47 (Cq, C9), 124.03 (CH, C8), 118.01 (CH, C1), 117.23 (CH, C6), 114.42 (CH, C7), 37.08 (CH₃, N2 CH₃). FT-IR (ATR, ν , cm⁻¹): 3112, 3092, 3064, 1951, 1814, 1783, 1686, 1580, 1542, 1507, 1448, 1375, 1346, 1323, 1263, 1214, 1188, 1149, 1073, 1033, 784, 736, 615. Anal. Calcd for C₈H₉N₂I (%): C, 36.95; H, 3.49; N, 10.77. Found (%): C, 37.21; H, 3.59; N, 10.89.

2-Ethylimidazo[1,5-*a*]pyridin-2-ium iodide (8) (C₉H₁₁N₂I). Starting materials: ethyl iodide (2.31 g, 14.81 mmol) and **2** (0.35 g, 2.96 mmol). Yield 0.7 g (2.55 mmol, 86%); yellow hygroscopic solid. ¹H NMR (300 MHz, DMSO-*d*₆, δ , ppm): 9.79 (s, 1H, H3), 8.62 (d, *J* = 6.8 Hz, 1H, H5), 8.32 (s, 1H, H1), 7.88 (d, *J* = 9.2 Hz, 1H, H8), 7.39–7.12 (m, 2H, overlapping signals for H6, H7), 4.55 (q, *J* = 7.3 Hz, 2H N2 CH₂ Me), 1.57 (t, *J* = 7.3 Hz, 3H N2 CH₂ CH₃). ¹³C NMR (75 MHz, DMSO-*d*₆, δ , ppm): 129.15 (CH, C3), 126.08 (CH, C5), 124.48 (Cq, C9), 124.12 (CH, C8), 118.08 (CH, C1), 117.24 (CH, C6), 112.94 (CH, C7), 45.47 (CH₂ N2 CH₂ Me) 15.37 (CH₃, N2 CH₂ CH₃). FT-IR (ATR, ν , cm⁻¹): 3113, 3087, 3062, 2937, 2878, 1652, 1544, 1450, 1376, 1336, 1314, 1221, 1152, 1125, 808, 788, 741, 618. Anal. Calcd for C₉H₁₁N₂I (%): C, 39.44; H, 4.05; N, 10.22. Found (%): C, 39.64; H, 4.15; N, 10.32.

2-Benzylimidazo[1,5-*a*]pyridin-2-ium bromide (9) (C₁₄H₁₃BrN₂). Starting materials: benzyl bromide (2.53 g, 14.8 mmol) and **2** (0.35 g, 2.96 mmol). Yield 0.66 g (2.28 mmol, 77%); green solid. ¹H NMR (300 MHz, DMSO-*d*₆, δ , ppm): 9.97 (d, *J* = 1.3 Hz, 1H, H3), 8.67 (dd, *J* = 6.8, 1.2 Hz, 1H, H5), 8.34 (dd, *J* = 1.4, 1.3 Hz, 1H, H1), 7.96–7.79 (m, 1H, H8), 7.65–7.32 (m, 2H, overlapping signals for H6, H7), 7.32–7.12 (m, 5H, overlapping signals for N2 CH₂ Ph), 5.83 (s, 2H N2 CH₂ Ph). ¹³C NMR (75 MHz, DMSO-*d*₆, δ , ppm): 134.59 (C_{Phenyl}, C2), 129.45 (CH, C3), 128.96 (C_{Phenyl}, H, 2C, overlapping signals for C4', C6'), 128.64 (C_{Phenyl}, H, 2C, overlapping signals for C3', C7'), 126.40 (CH, C5), 124.74 (CH, C8), 124.38 (Cq, C9), 118.17 (CH, C1), 117.37 (CH, C6), 113.29 (CH, C7), 52.94 (CH₂ N2 CH₂ Ph, C1'). FT-IR (ATR, ν , cm⁻¹): 3112, 3086, 3071, 2970, 2953, 1652, 1539, 1497, 1455, 1379, 1347, 1325, 1206, 1188, 1144, 1125, 1035, 835, 808, 759, 702, 686, 642. MS (ESI): *m/z* (%): 210 (19), 209 (100) [M – Br⁻], 183 (14), 182 (88). Anal. Calcd for C₁₄H₁₃N₂Br (%): C, 58.15; H, 4.53; N, 9.69. Found (%): C, 59.10; H, 4.72; N, 9.59.

2,5-Dimethylimidazo[1,5-*a*]pyridin-2-ium iodide (10) (C₉H₁₁IN₂). Starting materials: methyl iodide (1.07 g, 7.5 mmol) and 5-methylimidazo[1,5-*a*]pyridine (**6**; 0.2 g, 1.51 mmol). Yield 0.3 g (1.09 mmol, 72%); pale yellow solid. ¹H NMR (300 MHz, DMSO-*d*₆, δ , ppm): 9.81 (dd, *J* = 1.5, 0.7 Hz, 1H, H3), 8.25 (d, *J* = 1.8 Hz, 1H, H1), 7.86–7.71 (m, 1H, H8), 7.26 (dd, *J* = 9.2, 6.8 Hz, 1H, H7), 7.07 (dd, *J* = 6.8, 1.1 Hz, 1H, H6), 4.20 (s, 3H, N2 CH₃), 2.64

(s, 3H, C5 CH₃). ¹³C NMR (75 MHz, DMSO-*d*₆, δ, ppm): 135.57 (Cq, C5), 134.68 (CH, C3), 129.26 (Cq, C9), 129.02 (CH, C8), 120.37 (CH, C1), 116.04 (CH, C6), 111.32 (CH, C7), 35.12 (CH₃, N2 CH₃), 18.09 (CH₃ C5 CH₃) ppm. FT-IR (ATR, ν, cm⁻¹): 3114, 3091, 3074, 1941, 1812, 1785, 1676, 1578, 1541, 1449, 1385, 1348, 1327, 1266, 1212, 1186, 1146, 1068, 1033, 783, 735, 617. (+) MS (ESI): *m/z* (%): 147 (100) [(M - I⁻)⁺]. Anal. Calcd for C₉H₁₁N₂ (%): C, 39.44; H, 4.05; N, 10.22. Found (%): C, 39.78; H, 3.98; N, 10.18.

2-(2-Hydroxyethyl)imidazo[1,5-*a*]pyridin-2-ium iodide (11) (C₉H₁₁N₂O). Starting materials: 2-iodoethanol (0.9 ml, 11.51 mmol) and **2** (250 mg, 2.11 mmol). Yield 0.4 g (1.37 mmol, 65%); colourless solid. ¹H NMR (300 MHz, DMSO-*d*₆, δ, ppm): 9.75 (s, 1H, H3), 8.64 (d, *J* = 7.1 Hz, 1H, H5), 8.27 (s, 1H, H1), 7.91 (d, *J* = 9.5 Hz, 1H, H8), 7.41–7.13 (m, 2H, overlapping signals for H6, H7), 5.22 (d, *J* = 5.4 Hz, 1H OH), 4.64–4.49 (m, 2H, N2 CH₂ CH₂ OH), 3.86 (t, *J* = 5.2 Hz, 2H, N2 CH₂ CH₂). ¹³C NMR (75 MHz, DMSO-*d*₆, δ, ppm): 129.04 (CH, C3), 126.66 (CH, C5), 124.42 (Cq, C9), 124.02 (CH, C8), 118.18 (CH, C1), 117.33 (CH, C6), 113.68 (CH, C7), 59.64 (CH₂, N2 CH₂ CH₂ OH), 52.97 (CH₂, N2 CH₂ CH₂). FT-IR (ATR, ν, cm⁻¹): 3284, 3138, 3114, 3084, 2979, 1654, 1541, 1460, 1421, 1350, 1330, 1307, 1145, 1126, 1083, 1063, 945, 882, 797, 754, 662, 639. MS (EI): *m/z* (%): 163 (100) [(M - I⁻)]. Anal. Calcd for C₉H₁₁N₂O (%): C 37.26; H, 3.82; N, 9.66. Found (%): C, 37.63; H, 3.59; N, 9.42.

General Procedure for Synthesis of Gold(I)–NHC Complexes (12–16)

The respective imidazo[1,5-*a*]pyridin-2-ium halide salts (1 equiv.) **7–11** were suspended in dry dichloromethane and treated with Ag₂O (0.5 equiv.) with stirring for 5 h at ambient temperature in the dark. AuCl(SMe₂) (1 equiv.) was added and the mixture was stirred for another 10 h. The obtained suspension was filtered through celite (281 nm particle size), and the solvent was removed under reduced pressure to afford the desired products.

Chloro(2-methylimidazo[1,5-*a*]pyridin-3-ylidene)gold(I) (12) (C₈H₈N₂AuCl). Compound **7** (0.1 g, 0.384 mmol) was dissolved in dichloromethane and treated with Ag₂O (0.044 g, 0.192 mmol) for 5 h at ambient temperature in the dark. AuCl(SMe₂) (0.113 g, 0.384 mmol) was added, and the reaction was stirred for another 10 h. The product was purified using a celite column (281 nm particle size). Yield 0.065 g (0.178 mmol, 46%); colourless solid. ¹H NMR (600 MHz, CDCl₃-*d*, δ, ppm): 8.48 (dddd, *J* = 7.4, 1.1, 1.0, 1.0 Hz, 1H, H5), 7.33 (ddd, *J* = 9.3, 1.1, 1.1 Hz, 1H, H8), 7.25 (d, *J* = 0.7 Hz, 1H, H1), 6.92 (ddd, *J* = 9.3, 6.5, 0.9 Hz, 1H, H7), 6.70 (ddd, *J* = 7.4, 6.5, 1.2 Hz, 1H, H6), 4.11 (s, 3H, N2 CH₃). ¹³C NMR (150 MHz, CDCl₃-*d*, δ, ppm): 163.11 (C_{carbener}, C3), 130.37 (CH, C5), 127.43 (Cq, C9), 123.71 (CH, C8), 117.06 (CH, C1), 114.15 (CH, C6), 111.45 (CH, C7), 39.47 (CH₃, N2 CH₃). FT-IR (ATR, ν, cm⁻¹): 3207, 3114, 3054, 2924, 2851, 1919, 1649, 1464, 1341, 1307, 1250, 1171, 1094, 991, 931, 844, 750, 728, 637. MS (EI): *m/z* (%): 366 (33) [M (³⁷Cl)], 364 (100) [M (³⁵Cl)], 330 (10), 329 (98) [M - Cl⁻]. Anal. Calcd for C₈H₈N₂AuCl (%): C, 26.36; H, 2.21; N, 7.68. Found (%): C, 26.20; H, 2.49; N, 7.07.

Chloro(2-ethylimidazo[1,5-*a*]pyridin-3-ylidene)gold(I) (13) (C₉H₁₀N₂AuCl). Compound **8** (0.1 g, 0.264 mmol) was dissolved in dichloromethane and treated with Ag₂O (0.030 g, 0.132 mmol) for 5 h at ambient temperature in the dark. AuCl(SMe₂) (0.077 g, 0.264 mmol) was added, and the reaction mixture was stirred for another 10 h. The product was purified using a celite column (281 nm particle size). Yield 0.05 g (0.132 mmol, 50%); pale yellow solid. Single crystals suitable for X-ray measurements were grown by slow diffusion of diethyl ether into a solution of **13** in a

dichloromethane-*n*-hexane-acetonitrile mixture. ¹H NMR (300 MHz, CDCl₃-*d*, δ, ppm): 8.44 (dddd, *J* = 7.3, 1.1, 1.0, 1.0 Hz, 1H, H5), 7.51–7.28 (m, 2H, overlapping signals for H8, H1), 6.91 (ddd, *J* = 9.3, 6.6, 1.1 Hz, 1H, H7), 6.84–6.63 (m, 1H, H6), 4.48 (q, *J* = 7.3 Hz, 2H, N2 CH₂ Me), 1.59 (t, *J* = 7.3 Hz, 3H, N2 CH₂ CH₃). ¹³C NMR (75 MHz, CDCl₃-*d*, δ, ppm): 161.83 (C_{carbener}, C3), 130.35 (CH, C5), 127.41 (Cq, C9), 123.46 (CH, C8), 117.27 (CH, C1), 114.07 (CH, C6), 109.81 (CH, C7), 47.77 (CH₂, N2 CH₂ Me), 16.79 (CH₃, N2 CH₂ CH₃) ppm. FT-IR (ATR, ν, cm⁻¹): 3204, 3156, 3115, 2979, 2929, 2851, 1922, 1783, 1749, 1649, 1558, 1523, 1462, 1443, 1411, 1334, 1305, 1242, 1167, 1063, 980, 926, 799, 747, 730, 641. MS (EI): *m/z* (%): 380 (28) [M (³⁷Cl)], 378 (100) [M (³⁵Cl)], 343 (60) [M - Cl⁻], 314 (38), 118 (77), 117 (30). Anal. Calcd for C₉H₁₀N₂AuCl (%): C, 28.55; H, 2.66; N, 7.40. Found (%): C, 28.84; H, 2.77; N, 7.68.

Chloro(2-benzylimidazo[1,5-*a*]pyridin-3-ylidene)gold(I) (14) (C₁₄H₁₂N₂AuCl). Compound **9** (0.1 g, 0.347 mmol) in CH₂Cl₂ was treated with Ag₂O (0.04 g, 0.173 mmol) with stirring for 5 h. AuCl(SMe₂) (0.1 g, 0.347 mmol) was added and the reaction was stirred for another 10 h. The product was purified using a celite column (281 nm particle size). Yield 0.065 g (0.145 mmol, 42%); dark green solid. ¹H NMR (300 MHz, CDCl₃-*d*, δ, ppm): 8.49 (dddd, *J* = 7.3, 1.1, 1.0, 1.0 Hz, 1H, H3), 7.90 (s, 1H, H5), 7.38–7.26 (m, 5H, overlapping signals for N2 CH₂ Ph), 7.18–7.16 (m, 1H, H8), 6.90 (ddd, *J* = 9.4, 6.6, 1.1 Hz, 1H, H7), 6.69 (ddd, *J* = 7.3, 6.6, 1.2 Hz, 1H, H6), 5.60 (s, N2 CH₂ Ph). ¹³C NMR (75 MHz, DMSO-*d*₆, δ, ppm): 162.57 (C_{carbener}, C3), 134.64 (C_{phenyl}, C2'), 130.67 (CH, C5), 129.15 (C_{phenyl}, H, 2C, overlapping signals for C4', C6'), 128.99 (Cq, C9), 128.28 (C_{phenyl}, H, 2C, overlapping signals for C3', C7'), 127.51 (C_{phenyl}, H, C5'), 123.73 (CH, C8), 117.28 (CH, C1), 114.24 (CH, C6), 110.18 (CH, C7), 56.44 (CH₂, N2 CH₂ Ph, C1'). FT-IR (ATR, ν, cm⁻¹): 3207, 3145, 3086, 3032, 2929, 2852, 1650, 1525, 1494, 1454, 1394, 1364, 1343, 1322, 1248, 1206, 1079, 1062, 987, 847, 754, 711, 649. MS (EI): *m/z* (%): 442 (10) [M (³⁷Cl)], 440 (25) [M (³⁵Cl)], 405 (5) [M - Cl⁻], 314 (12), 207 (52), 208 (12), 91 (100) [Bn⁺]. Anal. Calcd for C₁₄H₁₂N₂AuCl (%): C, 38.16; H, 2.74; N, 6.36. Found (%): C, 37.42; H, 2.68; N, 6.51.

Chloro(2,5-dimethylimidazo[1,5-*a*]pyridin-3-ylidene)gold(I) (15) (C₉H₁₀N₂AuCl). Compound **10** (100 mg, 0.364 mmol) in CH₂Cl₂ (10 ml) was treated with Ag₂O (42.17 mg, 0.182 mmol) with stirring for 5 h at ambient temperature in the dark. AuCl(SMe₂) (116.69 mg, 0.364 mmol) was added and the mixture was stirred overnight at ambient temperature. The product was purified using a celite column (265 nm particle size). Yield 0.556 g (0.147 mmol, 40%); colourless solid. ¹H NMR (300 MHz, CDCl₃-*d*, δ, ppm): 7.41–7.24 (m, 1H, H8), 7.39 (s, 1H, H1), 6.88 (ddd, *J* = 9.3, 6.6, 0.4 Hz, 1H, H7), 6.49 (dd, *J* = 6.6, 1.2 Hz, 1H, H6), 4.21 (s, 3H, N2 CH₃), 3.24 (s, 3H, C5 CH₃). ¹³C NMR (75 MHz, CDCl₃-*d*, δ, ppm): 162.00 (C_{carbener}, C3), 134.10 (Cq, C5), 126.10 (Cq, C9), 122.64 (CH, C8), 115.34 (CH, C1), 114.78 (CH, C6), 112.15 (CH, C7), 40.37 (CH₃, N2 CH₃), 23.23 (CH₃, C5; CH₃). FT-IR (ATR, ν, cm⁻¹): 3206, 3064, 2929, 2817, 1653, 1472, 1337, 1306, 1251, 1169, 1084, 989, 933, 844, 748, 729, 636. MS (EI): *m/z* (%): 380 (30) [M (³⁷Cl)], 378 (87) [M (³⁵Cl)], 342 (100) [M - Cl⁻], 146 (82), 131 (35), 93 (25), 55 (28). Anal. Calcd for C₉H₁₀N₂AuCl (%): C, 28.55; H, 2.66; N, 7.40. Found (%): C, 28.76; H, 2.68; N, 7.49.

Bis(2-(2-hydroxyethyl)imidazo[1,5-*a*]pyridin-3-ylidene)gold(I) chloride (16) (C₁₈H₂₀N₄O₂AuCl). Compound **11** (0.06 g, 0.206 mmol) in CH₂Cl₂ (5 ml) was treated with Ag₂O (0.024 g, 0.103 mmol) with stirring for 5 h at ambient temperature in the dark. AuCl(SMe₂) (0.061 g, 0.206 mmol) was added and the mixture was stirred overnight. The product was purified using a celite column (265 nm particle size). Yield 0.054 g (0.097 mmol, 47%); colourless solid. ¹H NMR (600 MHz, DMSO-*d*₆, δ, ppm): 8.81 (dd, *J* = 7.1, 1.0 Hz, 1H, H5), 8.55 (dd, *J* = 7.1, 1.1 Hz, 1H, H5'), 8.05 (d,

$J = 1.1$ Hz, 1H, H1'), 7.97 (d, $J = 1.1$ Hz, 1H, H1), 7.72 (m, 2H, overlapping signals for H8, H8'), 7.21–6.82 (m, 4H, overlapping signals for H6, H6', H7, H7'), 5.18 (bs, 2H, ;CH₂:OH), 4.63–4.50 (m, 4H, overlapping signals for N2;CH₂;CH₂;OH, N2';CH₂;CH₂;OH), 4.03–3.91 (m, 4H, overlapping signals for N2;CH₂;CH₂, N2';CH₂;CH₂). ¹³C NMR (150 MHz, DMSO-*d*₆, δ , ppm): 174.61 (C_{carbonyl}, C3), 174.53 (C_{carbonyl}, C3'), 129.68 (CH, C5), 129.02 (CH, C5'), 127.00 (Cq, C9), 126.19 (Cq, C9), 123.12 (CH, C8), 122.98 (CH, C8), 117.95 (CH, C1), 117.91 (CH, C1), 114.80 (CH, C6), 114.74 (CH, C6'), 113.69 (CH, C7), 112.93 (CH, C7), 60.91 (CH₂, N2;CH₂;CH₂:OH), 60.40 (CH₂, N2';CH₂;CH₂:OH), 54.67 (CH₂, N2';CH₂;CH₂), 54.24 (CH₂, N2;CH₂;CH₂). FT-IR (ATR, ν , cm⁻¹): 3134, 3108, 2942, 2907, 2875, 1935, 1650, 1461, 1415, 1347, 1315, 1198, 1154, 1068, 1043, 929, 749, 732, 675, 657. (+) MS (ESI) m/z (%): 521 (100) [(M - Cl⁻)⁺], 522 (22). Anal. Calcd for C₁₈H₂₀N₄O₂AuCl (%): C, 38.69; H, 3.97; N, 10.03. Found (%): C, 37.94; H, 3.35; N, 10.67.

General Procedure for Synthesis of Silver(I)-NHC Complexes (17–20)

The respective salts **7–9** and **11** (1 equiv.) were dissolved in dichloromethane (20 ml) and treated with silver(I) acetate (2 equiv.) under reflux for 6–8 h in the dark. The resulting suspension was filtered over celite, and the solvent was removed under high vacuum to afford complexes **17–20** as colourless sticky solids.

(2-Methylimidazo[1,5-*a*]pyridin-3-ylidene)silver(I) acetate (17) (C₁₀H₁₁N₂O₂Ag). Starting materials: **7** (0.1 g, 0.384 mmol) and silver(I) acetate (0.132 g, 0.788 mmol). Yield 0.05 g (0.168 mmol, 43%); colourless sticky solid. ¹H NMR (300 MHz, DMSO-*d*₆, δ , ppm): 8.45 (dd, $J = 7.2$, 0.8 Hz, 1H, H5), 7.85 (s, 1H, H1), 7.56 (d, $J = 9.2$ Hz, 1H, H8), 6.97 (ddd, $J = 9.2$, 6.5, 0.7 Hz, 1H, H7), 6.77 (ddd, $J = 7.2$, 6.5, 1.1 Hz, 1H, H6), 4.08 (s, 3H, N2;CH₃), 1.86 (s, 3H, ;COCH₃, acetate). ¹³C NMR (75 MHz, DMSO-*d*₆, δ , ppm): 174.18 (C_{carbonyl}, C3), 170.33 (Cq, C_{carbonyl}, acetate), 130.48 (CH, C5), 128.05 (Cq, C9), 122.78 (CH, C8), 117.60 (CH, C1), 113.97 (CH, C6), 113.52 (CH, C7), 39.42 (CH₃, ;N2;CH₃), 22.64 (CH₃, ;O;CO;CH₃). FT-IR (ATR, ν , cm⁻¹): 3130, 3099, 2984, 2974, 1715, 1648, 1566, 1393, 1248, 1154, 1012, 769. (+) MS (ESI) m/z (%): 241.0 (90) [M^{(109)Ag} - OAc], 239.0 (100) [M^{(107)Ag} - OAc]. (-) MS (ESI) m/z (%): 299.0 (35) [M^{(109)Ag} - H⁺], 297.0 (40) [M^{(107)Ag} - H⁺], 255.0 (95), 253 (100), 241 (10), 239 (10), 131 (30) [(M - H⁺) - AgOAc]. Anal. Calcd for C₁₀H₁₁N₂O₂Ag (%): C, 40.16; H, 3.71; N, 9.37. Found (%): C, 40.40; H, 3.97; N, 9.10.

(2-Ethylimidazo[1,5-*a*]pyridin-3-ylidene)silver(I) acetate (18) (C₁₁H₁₃N₂O₂Ag). Starting materials: **8** (0.1 g, 0.364 mmol) and silver(I) acetate (0.125 g, 0.747 mmol). Yield 0.06 g (0.192 mmol, 52%); colourless sticky solid. ¹H NMR (300 MHz, DMSO-*d*₆, δ , ppm): 8.46 (dd, $J = 7.3$, 1.1 Hz, 1H, H5), 7.94 (d, $J = 1.1$ Hz, 1H, H1), 7.56 (ddd, $J = 9.3$, 1.2, 1.2 Hz, 1H, H8), 6.97 (ddd, $J = 9.3$, 6.5, 1.0 Hz, 1H, H7), 6.77 (ddd, $J = 7.3$, 6.5, 1.2 Hz, 1H, H6), 4.42 (q, $J = 7.3$ Hz, 2H, N2;CH₂;Me), 1.85 (s, 3H, ;CO;CH₃), 1.48 (t, $J = 7.3$ Hz, 3H, N2;CH₂;CH₃). ¹³C NMR (75 MHz, DMSO-*d*₆, δ , ppm): 174.44 (C_{carbonyl}, C3), 169.36 (Cq, C_{carbonyl}, acetate), 130.49 (CH, C5), 128.25 (Cq, C9), 122.73 (CH, C8), 117.71 (CH, C1), 113.98 (CH, C6), 111.94 (CH, C7), 47.47 (CH₂, ;N2;CH₂;Me), 22.81 (CH₃, ;O;CO;CH₃), 17.09 (CH₃, N2;CH₂;CH₃). FT-IR (ATR, ν , cm⁻¹): 3123, 2984, 2974, 1654, 1588, 1565, 1397, 1373, 1237, 1151, 1044, 1009, 749, 652. (+) MS (ESI) m/z (%): 255.0 (95) [M^{(109)Ag} - OAc], 253.0 (100) [M^{(107)Ag} - OAc]. (-) MS (ESI) m/z (%): 313.0 (35) [M^{(109)Ag} - H⁺], 311.0 (40) [M^{(107)Ag} - H⁺], 269.0 (95), 267.0 (100), 145.1 (30) [(M - H⁺) - AgOAc]. Anal. Calcd for C₁₁H₁₃N₂O₂Ag (%): C, 42.40; H, 4.19; N, 8.95. Found (%): C, 40.64; H, 4.44; N, 8.68.

(2-Benzylimidazo[1,5-*a*]pyridin-3-ylidene)silver(I) acetate (19) (C₁₆H₁₅N₂O₂Ag). Starting materials: **9** (0.1 g, 0.347 mmol) and silver(I) acetate (0.118 g, 0.711 mmol). Yield 0.065 g (0.173 mmol, 50%); colourless sticky solid; single crystals of complex **19** in dichloromethane/*n*-hexane mixture. ¹H NMR (300 MHz, DMSO-*d*₆, δ , ppm): 8.47 (dd, $J = 7.2$, 1.1 Hz, 1H, H5), 7.98 (s, 1H, H3), 7.56 (d, $J = 9.2$ Hz, 1H, H8), 7.52–7.28 (m, 5H, overlapping signals for ;N2;CH₂;Ph), 6.98 (ddd, $J = 9.2$, 6.5, 0.7 Hz, 1H, H7), 6.80 (ddd, $J = 7.2$, 6.5, 1.1 Hz, 1H, H6), 5.63 (s, 2H, ;N2;CH₂;Ph), 1.87 (s, 3H, ;COCH₃). ¹³C NMR (75 MHz, DMSO-*d*₆, δ , ppm): 174.99 (C_{carbonyl}, C3), 170.00 (Cq, C_{carbonyl}, acetate), 136.84 (C_{phenyl}, C2), 130.82 (CH, C5), 128.76 (C_{phenyl}H, 2C, overlapping signals for C4', C6'), 128.31 (Cq, C9), 128.18 (C_{phenyl}H, C5'), 128.07 (C_{phenyl}H, 2C, overlapping signals for C3', C7'), 122.99 (CH, C8), 117.80 (CH, C1), 114.20 (CH, C6), 112.54 (CH, C7), 55.54 (CH₂, ;N2;CH₂;Ph, C1'), 23.07 (CH₃, ;O;CO;CH₃). FT-IR (ATR, ν , cm⁻¹): 3134, 3108, 2923, 2853, 1571, 1389, 1335, 1155, 1053, 923, 773, 719, 672, 617. (+) MS (ESI) m/z (%): 317.0 (95) [M^{(109)Ag} - OAc], 315.0 (100) [M^{(107)Ag} - OAc]. (-) MS (ESI) m/z (%): 375.0 (65) [M^{(109)Ag} - H⁺], 373.0 (70) [M^{(107)Ag} - H⁺], 331.0 (95), 329.0 (100), 207.1 (25) [(M - H⁺) - AgOAc]. Anal. Calcd for C₁₆H₁₅N₂O₂Ag (%): C, 51.22; H, 4.03; N, 7.47. Found (%): C, 51.58; H, 4.12; N, 7.58.

2-((2-Hydroxyethyl)imidazo[1,5-*a*]pyridin-3-ylidene)silver(I) acetate (20) (C₁₁H₁₃N₂O₂Ag). Starting materials: **11** (0.1 g, 0.344 mmol) and silver(I) acetate (0.118 g, 0.706 mmol). Yield 0.065 g (0.198 mmol, 50%); colourless sticky solid. ¹H NMR (300 MHz, DMSO-*d*₆, δ , ppm): 8.63 (dd, $J = 7.4$, 1.1 Hz, 1H, H5), 8.06–7.76 (m, 1H, H1), 7.62 (ddd, $J = 9.3$, 1.2, 1.2 Hz, 1H, H8), 7.01 (ddd, $J = 7.4$, 6.4, 1.1 Hz, 1H, H6), 6.92–6.76 (m, 1H, H7), 4.62–4.44 (m, 3H, CH₂;CH₂:OH), 4.01–3.79 (m, 2H, N2;CH₂;CH₂), 1.89 (s, 3H, ;COCH₃). ¹³C NMR (75 MHz, DMSO-*d*₆, δ , ppm): 173.97 (C_{carbonyl}, C3), 170.18 (Cq, C_{carbonyl}, acetate), 130.21 (CH, C5), 128.42 (Cq, C9), 122.66 (CH, C8), 117.76 (CH, C1), 113.96 (CH, C6), 113.17 (CH, C7), 61.09 (CH₂, N2;CH₂;CH₂:OH), 55.15 (CH₂, N2;CH₂;CH₂), 23.98 (CH₃, ;O;CO;CH₃). FT-IR (ATR, ν , cm⁻¹): 3253, 3162, 3133, 2918, 2848, 1649, 1568, 1555, 1389, 1334, 1248, 1171, 1083, 1040, 838, 760, 669. (+) MS (ESI) m/z (%): 271.0 (90) [M^{(109)Ag} - OAc], 269.0 (100) [M^{(107)Ag} - OAc]. (-) MS (ESI) m/z (%): 329.0 (70) [M^{(109)Ag} - H⁺], 327.0 (75) [M^{(107)Ag} - H⁺], 287.0 (95), 285.0 (100), 161.1 (20) [(M - H⁺) - AgOAc]. Anal. Calcd for C₁₁H₁₃N₂O₂Ag (%): C 40.15; H, 3.98; N, 8.51. Found (%): C, 40.55; H, 4.01; N, 8.62.

X-ray Diffraction Studies

Data were recorded at 100(2) K using an Oxford Diffraction Nova A diffractometer with monochromated Cu K α radiation. The structures were refined anisotropically using the SHELXL-97 program. Hydrogen atoms were included as idealized methyl groups allowed to rotate but not tip, or placed geometrically and allowed to ride on their attached carbon atoms. For **19**, the acetate methyl group was rotationally disordered and was refined as an idealized hexagon of half-occupied hydrogen sites. The crystallographic data are summarized in Table 1.

Crystallographic data (excluding structure factors) for the structures reported in this paper have been deposited with the Cambridge Crystallographic Data Centre as supplementary publications no. CCDC-1430678 (**13**) and CCDC-1430679 (**19**). Copies of the data can be obtained free of charge on application to CCDC, 12 Union Road, Cambridge CB2 1EZ, UK (fax: (+44) 1223-336-033; www.ccdc.cam.ac.uk/data_request/cif).

Table 1. Crystallographic data

	13	19
Empirical formula	C ₉ H ₁₀ AuClN ₂	C ₁₆ H ₁₅ AgN ₂ O ₂
Formula weight	378.61	375.17
Temperature (K)	100(2)	100(2)
Wavelength, λ (Å)	1.54184	1.54184
Crystal system	Monoclinic	Monoclinic
Space group	<i>P</i> 2 ₁ / <i>c</i>	<i>P</i> 2 ₁ / <i>n</i>
<i>a</i> (Å)	8.0435(3)	8.7360(2)
<i>b</i> (Å)	15.9202(6)	15.3443(3)
<i>c</i> (Å)	7.6186(3)	10.7279(2)
β (°)	94.878(2)	93.330(2)
Volume (Å ³)	972.05(6)	1435.64(5)
<i>Z</i>	4	4
Reflections collected	20 005	17 374
Independent reflections	2013 ($R_{\text{int}} = 0.0720$)	2858 ($R_{\text{int}} = 0.0380$)
Goodness of fit on F^2	1.070	0.995
ρ_{calcd} (g cm ⁻³)	2.587	1.736
μ (mm ⁻¹)	30.575	11.313
$R(F_o)$ [$I > 2\sigma(I)$]	0.0326	0.0238
$R_w(F_o^2)$	0.0859	0.0662
$\Delta\rho$ (e Å ⁻³)	1.530/-1.798	0.453/-1.118

In Vitro Anti-tumour Activity towards Human Tumour Cell Lines

Anti-tumour activity of these compounds was tested in a mono-layer cell survival and proliferation assay using human tumour cell lines. Studies using panels of human tumour cell lines of different origin/histotype allow for analysis of potency and tumour selectivity of test compounds.

Ten out of the twelve cell lines as tested were established at Oncotest from patient-derived human tumour xenografts passaged subcutaneously in nude mice.^[27] The origin of the donor xenografts has been described.^[28,29] The other 16 cell lines were either provided by the National Cancer Institute (Bethesda, MA, USA) or were purchased from ATCC (Rockville, MD, USA) or DSMZ (Braunschweig, Germany). Cells were cultured in RPMI 1640 medium, supplemented with 10% foetal calf serum and 0.1 mg ml⁻¹ gentamicin under standard conditions (37 °C, 5% CO₂). Authenticity of all cell lines was proved by STR analysis at DSMZ (Braunschweig, Germany).

A modified propidium iodide assay was used to assess the activity of compounds towards human tumour cell lines.^[30] Briefly, cells were harvested from exponential phase cultures by trypsinization, counted and plated in 96-well flat-bottom microtiter plates at a cell density dependent on the cell line (4000–20 000 cells per well). After a 24 h recovery period to allow the cells to adhere and resume exponential growth, compounds were added at 10 concentrations in half-log increments and left for a further 4 days. The inhibition of proliferation was determined by measuring the DNA content using an aqueous propidium iodide solution (7 µg ml⁻¹). Fluorescence was measured using an Enspire Multimode-Plate Reader (excitation $\lambda = 530$ nm, emission $\lambda = 620$ nm), providing a direct relationship to the total viable cell number. In each experiment, all data points were determined in duplicate. Anti-tumour activity was reported as the absolute IC₅₀ value, which reflects the concentration of the test compound that achieves test/control values of 50%. Calculations were performed using a four-parameter nonlinear curve fit (Oncotest Data Warehouse software). The overall potency of a

compound was determined by the geometric mean IC₅₀ values of all individual IC₅₀ values. In the heatmap representation of IC₅₀ values, the distribution of values obtained for a test compound in the individual tumour models is given in relation to the geometric mean value, obtained over all cell lines tested.

The individual IC₅₀ values are highlighted in colours ranging from dark green ($\leq 1/32$ -fold geometric mean IC₅₀, corresponding to very potent compound activity or high tumour sensitivity) to dark red (≥ 32 -fold geometric mean IC₅₀, corresponding to lack of compound activity or tumour resistance). The heatmap representation, therefore, corresponds to an anti-proliferative 'fingerprint' profile of a test compound.

Results and Discussion

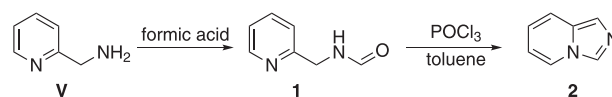
Imidazo[1,5-*a*]pyridine was prepared in two steps according to an established synthetic procedure,^[31] starting from commercially available pyridin-2-yl methanamine (**V**) (Scheme 1).

For complex **15**, we installed a substituent in the 5-position of the pyridine ring that points towards the metal upon coordination, and 5-methylimidazo[1,5-*a*]pyridine (**6**) is obtained in four steps (Scheme 2).^[32]

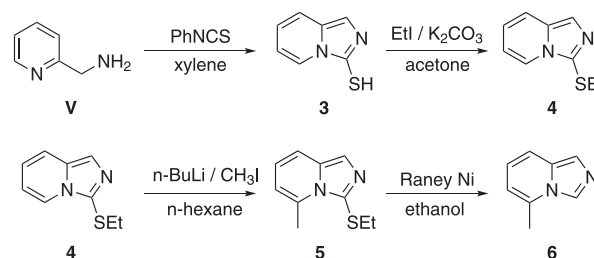
The desired imidazolium salts **7–11** were obtained by refluxing substrates **2** and **6** (Scheme 2) with an excess of the respective alkyl halides in THF. The NHC–gold(I) complexes were obtained by a ligand transfer reaction from 'silver–imidazopyridine' complexes that were generated *in situ* by treatment of salts **7–11** with Ag₂O, followed by reaction with chloro(dimethylsulfide)gold(I) in dichloromethane. Subsequent recrystallization from a dichloromethane/*n*-hexane mixture gave complexes **12–16** as off-white solids in 40–50% yields (Scheme 3).

However, for ligand **11**, the desired gold(I) chloride complex was obtained only in trace amounts; **16** was isolated instead and fully characterized (Scheme 4). The formation of complex **16** might be explained by the low solubility of **11** in dichloromethane. All NHC–gold(I) complexes were stable enough to be handled in air during the workup process.

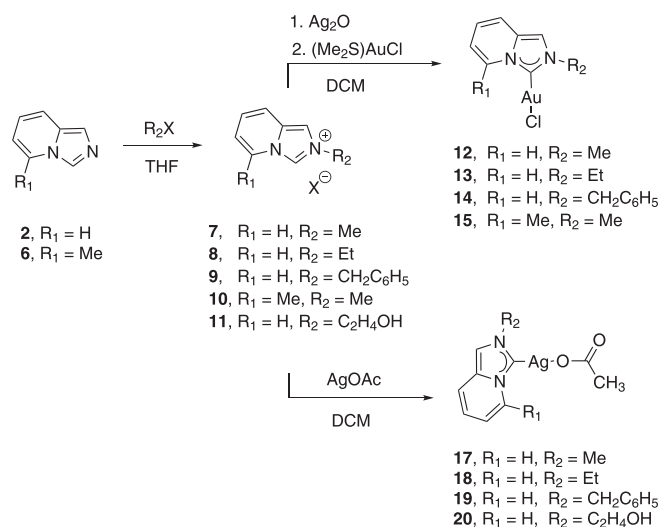
The *in situ* deprotonation of the imidazolium salts **7–9** and **11** with silver acetate in a 2:1 molar ratio in dichloromethane afforded the corresponding Ag(I)–NHC complexes in moderate yields (Scheme 3). The structures of all the metal complexes are presented in Fig. 3.



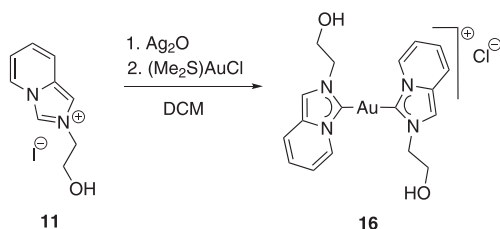
Scheme 1. Synthesis of imidazo[1,5-*a*]pyridine ligand (**2**).



Scheme 2. Synthesis of 5-methylimidazo[1,5-*a*]pyridine ligand (**6**).



Scheme 3. Synthesis of proligands **7–11** and of Au(I)–NHC complexes **12–15** and Ag(I)–NHC complexes **17–20**.



Scheme 4. Synthesis of complex **16**.

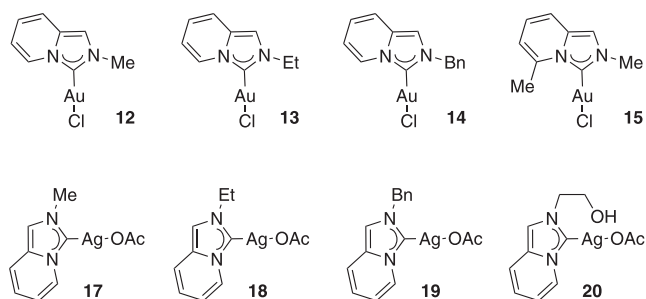


Figure 3. Structures of Au(I)Cl and Ag(I)OAc derivatives.

NMR Spectra and Molecular Structures

The conversion of salts **7–11** to the corresponding Au–NHC complexes is characterized by the disappearance in the ¹H NMR spectra of the imidazolium signals in the range 9.68–9.89 ppm. In the ¹³C NMR spectra, the characteristic resonance corresponding to the C (carbene) atom is detected at 163.11, 161.83, 162.57 and at 162.00 ppm, respectively, for **12**, **13**, **14** and **15**, confirming the formation of the NHC–gold(I) complexes.^[33] In agreement with previous data, the molecular ion peak [M⁺] dominates the EI-MS spectra of complexes **12–15**. In the case of complex **16**, the two C(carbene) resonances appear at 174.61 and 174.53 ppm, and the (+) ESI-MS is dominated by [(M – Cl)⁺] fragment peaks arising from the loss of the counter anion, which confirm the formation of the dicarbene gold(I) complex.

The solid structure of complex **13** was analysed using X-ray diffraction (Fig. 4). Compound **13** crystallizes in the monoclinic space group *P*₂₁/*c*. The structure of **13** shows no unexpected features. The molecule is planar within a root mean square deviation of 0.1 Å. The bond angle C2–Au–Cl is almost linear with a value of 177.78(17)° and is consistent with the average values of 177.10° and 179.13° for similar gold(I)–NHC complexes based on the imidazo[1,5-*a*]pyridine moiety.^[10,33]

The C–Au (1.997(6) Å) and Au–Cl (2.3170(12) Å) bond lengths are consistent with the average values of 1.988 and 2.290 Å, respectively, for 313 examples of the fragment C(carbene)–Au–Cl found in a CCDC search.^[34] Moreover, the C_{NHC}–Au bond length is comparable to that found in gold(I) complexes containing related NHC ligands.^[10,33]

Complexes **17–20** were obtained by treating salts **7–9** and **11** with two equivalents of silver acetate in dichloromethane in the absence of light. In all cases, after the removal of AgX (X = I, Br) by filtration and removal of the solvents in vacuum, the desired products were obtained in pure form and in good yields; no further purification was necessary. Complexes **17–20** were fully characterized using ¹H NMR and ¹³C NMR spectroscopy, mass spectrometry and elemental analysis. The solid structure of **19** was analysed using single-crystal X-ray diffraction (Figs 5, 6).

Complex **19** crystallizes in the monoclinic space group *P*₂₁/*n*. Adjacent linear (176.31(7)°) C–Ag–O units are connected via an argentophilic Ag...Ag contact^[35] (3.2692(3) Å) to form an inversion-symmetric dimer. The C–Ag (2.057(2) Å) and Ag–O (2.099(2) Å) bond distances again correspond well to the average values for 48 C(carbene)–Ag–O residues found in a CCDC search (2.067 and 2.130 Å).^[35] The dimers are further linked by a 'weak' but short contact H9...O2 (2.27 Å) to form corrugated layers parallel to (10). The C(carbene)–Ag bond length in compound **19** is comparable to that found in related NHC–silver(I) acetate complexes, and for instance, a caffeine-based NHC–silver acetate complex exhibits an Ag–C bond length of 2.067(3) Å.^[36]

The absence of the characteristic proton signal of imidazo[1,5-*a*]pyridin-2-ium salts at 9.68–9.97 ppm and the appearance of new resonances at 1.85–1.89 ppm for the acetate protons in all ¹H NMR spectra of complexes **17–20** indicate the successful formation of the desired silver complexes. In addition, the ¹³C NMR resonance

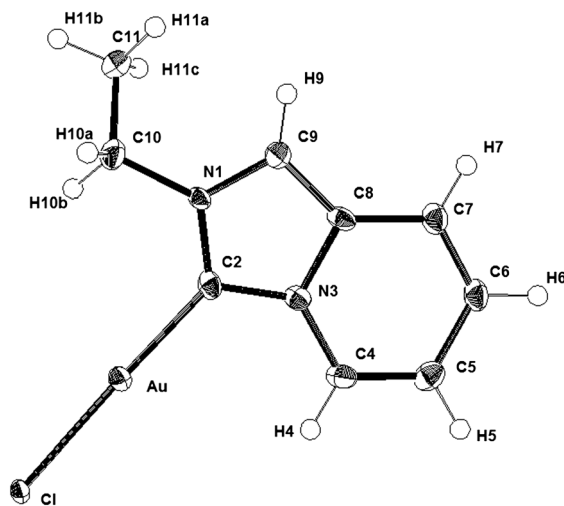


Figure 4. ORTEP representation of **13** with thermal displacement parameters drawn at 50% probability. Selected bond lengths (Å) and angles (°): Au–C2 1.997(6), Au–Cl 2.3170(12); C2–Au–Cl 177.78(17), N1–C2–N3 105.2(5), N1–C2–Au 129.4(4), N3–C2–Au 125.4(4).

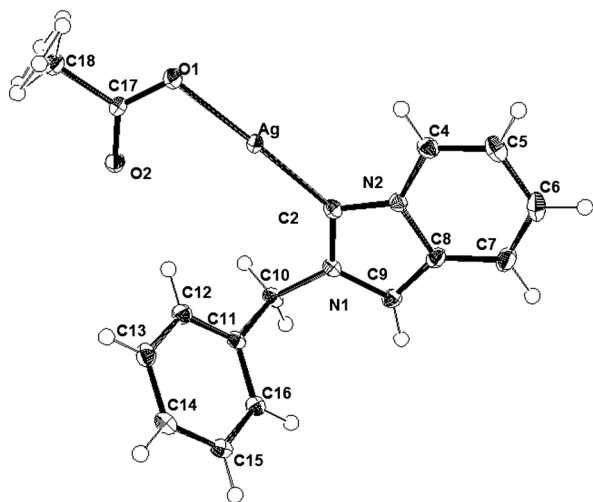


Figure 5. ORTEP representation of compound **19** with thermal displacement parameters drawn at 50% probability. Selected bond lengths (Å) and angles (°): Ag–C2 2.057(2), Ag–O1 2.0990(16), O1–C17 1.277(3), O2–C17 1.239(3), N1–C10 1.473(3), C10–C11 1.509(3), C17–C18 1.519(3); C2–Ag–O1 176.31(3), N1–C2–N2 103.15(7), C17–O1–Ag 11.73(13), N1–C10–C11 111.83(16), O2–C17–O1 124.7(2).

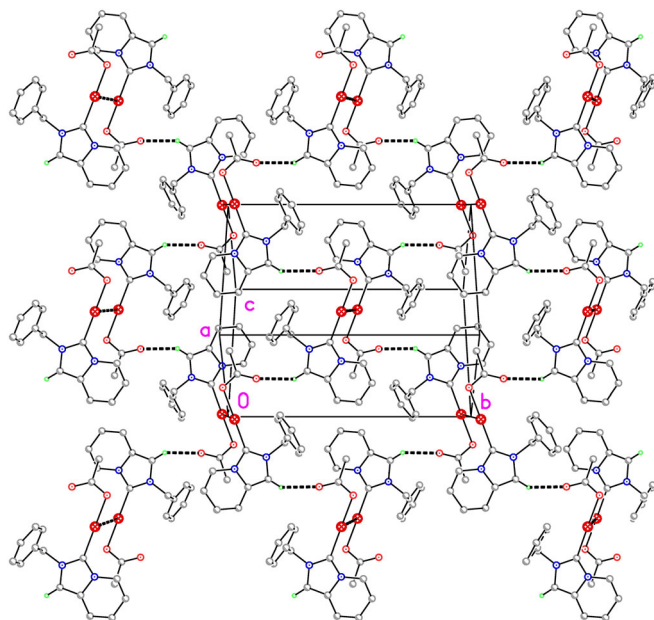


Figure 6. Packing diagram of compound **19** viewed perpendicular to $(10\bar{1})$. Dashed lines indicate Ag...Ag or H...O contacts.

of the carbene carbon atoms in complexes **17–20** appears in the range 173.97–174.99 ppm,^[36] whereas the imidazolium carbon resonance in the corresponding precursors **7–9** and **11** is found in the range 129.04–129.45 ppm. The ¹³C NMR spectra of complexes **17–20** also show the characteristic acetate resonances of the carbonyl and methyl carbon atoms in the range 169.36–170.33 and 22.64–23.98 ppm, respectively. In agreement with previous data, the (+) ESI-MS of all four NHC–silver(I) acetate complexes (**17–20**) are dominated by the $[(M - OAc)^+]$ fragment arising from the loss of one acetate ligand. Additionally, the identity of the complexes is also established by a base peak for the $[(M - H^+)]^-$ fragments in the (–) ESI-MS spectra.

Anti-tumour Activity

The *in vitro* anti-tumour activity of compounds **12–20** was assessed using a panel of 12 human tumour cell lines of 10 different cancer types with monolayer cell survival and proliferation assays (Fig. 7). The cell lines were derived from colon, gastric, lung, mammary, ovarian, pancreatic, uterine, renal and prostate cancers.

Among the target Au(I)–NHC complexes, compounds **13–15** exhibit good anti-tumour activity with mean IC_{50} values in the range 10.4–12.0 μ M, while compound **12** is clearly less active (mean IC_{50} = 57.5 μ M). Compound **12** was purified by column chromatography in order to test its stability and this could result in a decrease of its biological activity. The best cytotoxicity is recorded for **15** and **13** with mean IC_{50} values of 10.4 and 11.1 μ M, respectively. As depicted in Fig. 8 (heatmap representation), complex **15** shows good activity towards the prostate cancer cell line 22Rv1 (IC_{50} = 4.06 μ M) and the breast cancer cell line MAXF-401 (IC_{50} = 5.11 μ M). In addition good activity is detected towards the cell lines UXF-1138 (uterus; IC_{50} = 7.00 μ M), GFX-251 (stomach; IC_{50} = 7.23 μ M) and LXFL-529 (lung; IC_{50} = 8.53 μ M). Complex **13** shows excellent activity towards the cell lines LXFL-529 (lung; IC_{50} = 4.87 μ M), UXF-1138 (uterus; IC_{50} = 5.82 μ M) and MAXF-401 (breast; IC_{50} = 6.68 μ M).

A somewhat lower potency is detected for complexes **14** (IC_{50} = 12.0 μ M) and **19** (mean IC_{50} = 12.3 μ M). Compounds **16**, **17**, **18** and **20** show mean IC_{50} values in the range 17.0–22.8 μ M.

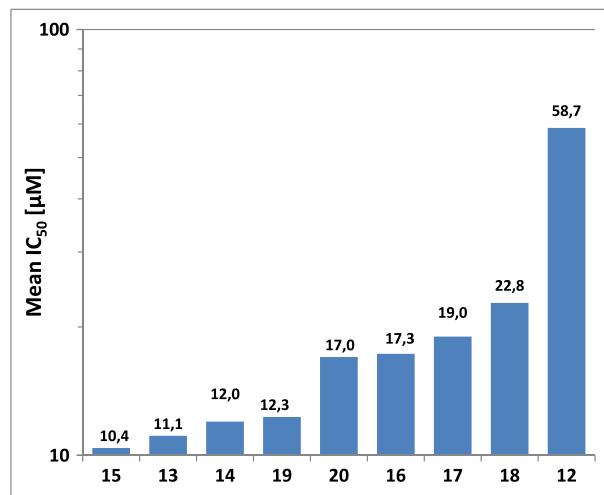


Figure 7. *In vitro* anti-tumour activity of compounds **12–20** in a panel of 12 human tumour cell lines (mean IC_{50} values).

compound	unit	Cell lines												Geom. mean IC_{50} [μ M]
		UXF-1138	GFX-251	LXFL-529	LXFL-529	MAXF-401	MERY-462	OVNF-899	PANF-1657	PRNF-22Rv1	PNF-1752	RNF-486	UXF-1138	
15	μ M	11.28	7.23	17.54	8.53	5.11	11.93	31.12	12.32	4.06	14.07	14.31	7.00	10.4
13	μ M	14.45	10.48	14.55	4.87	6.68	12.92	27.02	12.00	12.25	13.05	12.19	5.82	11.1
14	μ M	30.53	10.79	21.97	5.05	8.42	10.96	25.91	11.42	6.95	18.79	10.77	6.16	12.0
19	μ M	14.67	9.60	17.94	11.91	4.10	27.33	12.52	11.80	11.99	11.02	15.11	11.76	12.3
20	μ M	18.07	10.81	34.37	12.03	6.93	31.05	32.06	13.13	12.47	20.07	18.59	17.03	17.0
16	μ M	18.52	15.33	23.87	18.47	10.62	18.24	34.53	11.79	12.51	18.12	23.14	13.65	17.3
17	μ M	21.29	17.58	40.47	11.83	6.53	30.42	43.58	17.90	11.43	21.85	13.55	23.67	19.0
18	μ M	23.88	20.15	36.76	13.26	10.19	31.55	48.07	13.08	27.72	19.92	23.56	32.51	22.8
12	μ M	78.10	41.89	75.66	37.42	33.99	73.72	91.18	37.52	80.97	80.31	44.00	73.39	58.7

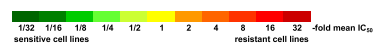


Figure 8. Heatmap representation of individual IC_{50} values of nine compounds (**12–20**) in a panel of 12 human tumour cell lines.

Complex **14**, with $IC_{50} = 11.97 \mu\text{M}$, shows a moderate activity against lung, uterus, prostate and breast cancer cell lines LXFL-529 ($IC_{50} = 5.05 \mu\text{M}$), UXF-1138 ($IC_{50} = 6.16 \mu\text{M}$), PRXF 22Rv1 ($IC_{50} = 6.95 \mu\text{M}$) and MAXF-401 ($IC_{50} = 8.42 \mu\text{M}$), respectively. However, complex **16** shows only moderate activity ($IC_{50} = 17.27 \mu\text{M}$) with sensitivity only towards the breast cancer cell line MAXF-401 ($IC_{50} = 10.623 \mu\text{M}$).

The activity profiles of gold(I)–NHC complexes **13–15** are quite similar to each other, indicating a similar mode of action, suggesting that the anti-tumour activity may intimately depend on the metal, on its ligands as an intact fragment and on the ligands themselves. In our case, changing the substituent groups at the heteroatom, CH_3 (compound **15**), C_2H_5 (compound **13**) or $\text{CH}_2\text{C}_6\text{H}_5$ (compound **14**), results in relatively small changes in the anti-tumour activity. On the other hand, the incorporation within the structure of a biologically active unit (1,2,4-oxadiazol, anthracene, indole, 2-pyridine, 2,3,4,5-tetra-*O*-acetyl- β -glucopyranose, etc.) may dramatically enhance the cytotoxicity (mean $IC_{50} < 0.1 \mu\text{M}$) and tumour selectivity, as was recently reported by our group.^[37]

Related gold–NHC complexes derived from imidazo[1,5-*a*]pyridine derivatives^[38] inhibited the growth of different cancer cell lines (HCT 116 colorectal carcinoma, Hep 62 human liver carcinoma, A 259 lung cancer with $IC_{50} = 4.73$ and $9.48 \mu\text{M}$) and induced apoptosis in B16F10 cells (mouse *Mus musculus*, $IC_{50} = 9.4 \mu\text{M}$). Our designed gold(I)–NHC complexes **12–16** preferentially inhibit breast and lung cancer cell lines MAXF-401 and LXFL-529 revealing a similar potency (mean $IC_{50} < 8.53 \mu\text{M}$).

Ag(I)–NHC complexes **17–20** show moderate to good activity. The lowest cytotoxicity is measured for complex **20** ($IC_{50} = 38.49 \mu\text{M}$) with sensitivity only against breast cancer cell line MAXF-401 ($IC_{50} = 11.90 \mu\text{M}$). Compound **17** exhibits very good toxicity also towards breast cancer cell line MAXF-401 ($IC_{50} = 6.53 \mu\text{M}$) with an overall IC_{50} value of $19.01 \mu\text{M}$. No significant change in the biological activity is observed when an ethyl substituent (compound **18**) is changed to a methyl substituent (**17**). However, complex **18** shows lower activity ($IC_{50} = 22.83 \mu\text{M}$), again with sensitivity against breast cancer cell line MAXF-401 ($IC_{50} = 10.19 \mu\text{M}$). The highest cytotoxicity is recorded for compound **19** ($IC_{50} = 12.28 \mu\text{M}$) with good inhibitory properties towards breast and stomach cancer cell lines MAXF-401 ($IC_{50} = 4.101 \mu\text{M}$) and GFX-251 ($IC_{50} = 9.599 \mu\text{M}$), respectively. Compound **20** also exhibits good activity ($IC_{50} = 16.99 \mu\text{M}$) with sensitivity against breast and stomach cancer cell lines MAXF-401 ($IC_{50} = 6.927 \mu\text{M}$) and GFX-251 ($IC_{50} = 10.81 \mu\text{M}$), respectively.

Even though similar silver(I)–NHC complexes based on the imidazo[1,5-*a*]pyridine moiety have not been studied so far, silver(I) acetate NHC complexes derived from the imidazole^[20]/benzimidazole core^[39] have been tested as anticancer agents. The imidazole complexes inhibit the growth of tumour cell lines, with preference for ovarian (OVCAR-3), breast (MCF-7) and colon (HT-29) carcinomas with IC_{50} values of around $10 \mu\text{M}$, while the benzimidazole complexes have activity against the renal cancer cell line Caki-1, with IC_{50} values in the range $5.4\text{--}25 \mu\text{M}$. Our silver(I) acetate complexes **17–20** show an increased cytotoxic activity against breast (MAXF-401) and stomach (GFX-251) cancer cell lines.

Conclusions

Two new series of unsymmetrically substituted gold(I) and silver(I) NHCs derived from imidazo[1,5-*a*]pyridines were synthesized from

the corresponding imidazolium salts. All derivatives were isolated, characterized and tested for *in vitro* anti-tumour activity towards a panel of 12 cell lines using a monolayer cell survival and proliferation assay. Four compounds revealed good potency and tumour selectivity, with individual IC_{50} values in the micromolar range, namely **15** (mean $IC_{50} = 10.4 \mu\text{M}$), **13** ($11.1 \mu\text{M}$), **14** ($12.0 \mu\text{M}$) and **19** ($12.3 \mu\text{M}$). All derivatives were obtained in high purity (at least 95%) and good to moderate yields. The structural assignments were corroborated using X-ray structure analysis for compounds **13** and **19**.

Acknowledgments

This work was supported by the Romanian National Authority for Scientific Research through the Exploratory Research Program IDEI-PCE-PROJECT no. 341-/05.10.2011 – Immunomodulatory Fluoroglycopeptide Molecular Architectures (I. Neda).

References

- [1] N. F. Ford, L. J. Browne, T. Campbell, C. Gemenden, R. Goldstein, C. Gude, J. W. Wasley, *J. Med. Chem.* **1985**, *28*, 164.
- [2] D. Kim, L. Wang, J. J. Hale, C. L. Lynch, R. J. Budhu, M. MacCoss, S. G. Mills, L. Malkowitz, S. L. Gould, J. A. Demartino, M. S. Springer, D. Hazuda, M. Miller, J. Kessler, R. C. Hrin, G. Carver, A. Carella, K. Henry, J. Lineberger, W. A. Schleif, E. A. Emini, *Bioorg. Med. Chem. Lett.* **2005**, *15*, 2129.
- [3] A. Kamal, G. Ramakrishna, P. Raju, A. V. Rao, A. Viswanath, V. L. Nayak, S. Ramakrishna, *Eur. J. Med. Chem.* **2011**, *46*, 2427.
- [4] B. W. Trotter, K. K. Nanda, C. S. Burgey, C. M. Potteiger, J. Z. Deng, A. I. Green, J. C. Hartnett, N. R. Kett, Z. Wu, D. A. Henze, K. D. Penna, R. Desai, M. D. Leitt, W. Lemaire, R. B. White, S. Yeh, M. O. Urban, S. A. Kane, G. D. Hartman, M. T. Bilodeau, *Bioorg. Med. Chem. Lett.* **2011**, *2*, 2354.
- [5] M. Nakatsuka, T. Shimamura, JP Patent 2001035664, **2001**. *Chem. Abstr.* **2001**, *134*, 93136.
- [6] H. Nakamura, H. Yamamoto, WO Patent 2005043630, **2005**. *Chem. Abstr.* **2005**, *142*, 440277.
- [7] a) M. Alcarazo, S. J. Roseblade, A. R. Cowley, R. Fernández, J. M. Brown, J. M. Lassaletta, *J. Am. Chem. Soc.* **2005**, *127*, 3290. b) C. Burstein, C. W. Lehmann, F. Glorius, *Tetrahedron* **2005**, *61*, 6207.
- [8] a) B. K. Rana, V. Bertolasi, S. Pal, P. Mitra, J. Dinda, *J. Mol. Struct.* **2013**, *1049*, 458. b) M. Espina, I. Rivilla, A. Conde, M. M. Díaz-Requejo, P. J. Pérez, E. Álvarez, R. Fernández, J. M. Lassaletta, *Organometallics* **2015**, *34*, 1328.
- [9] a) S. Würtz, F. Glorius, *Acc. Chem. Res.* **2008**, *41*, 1523. b) M. Nonnenmacher, D. Kunz, F. Rominger, T. J. Oeser, *J. Organomet. Chem.* **2007**, *692*, 2554. c) S. J. Roseblade, A. Ros, D. Monge, M. Alcarazo, E. Alvarez, J. M. Lassaletta, R. Fernández, *Organomet* **2007**, *26*, 2570. d) A. Fürstner, M. Alcarazo, H. Krause, C. W. Lehmann, *J. Am. Chem. Soc.* **2007**, *129*, 12676. e) D. Mishra, S. Naskar, B. Adhikary, R. J. Butcher, S. K. Chattopadhyay, *Polyhedron* **2005**, *24*, 201. f) C.-H. Chien, S. Fujita, S. Yamoto, T. Hara, T. Yamagata, M. Watanabe, K. Mashima, *Dalton Trans.* **2008**, 916.
- [10] a) J. Dinda, T. Samanta, A. Nandy, K. Das Saha, S. K. Seth, S. K. Chattopadhyay, C. W. Bielawski, *New J. Chem.* **2014**, *38*, 1218. b) B. K. Rana, A. Nandy, V. Bertolasi, C. W. Bielawski, K. Das Saha, J. Dinda, *Organometallics* **2014**, *33*, 2544. c) T. Samanta, R. N. Munda, G. Roymahapatra, A. Nandy, K. Das Saha, S. S. Al-Deyab, J. Dinda, *J. Organomet. Chem.* **2015**, *791*, 183.
- [11] a) G. R. Pettit, J. C. Collins, J. C. Knight, D. L. Herald, R. A. Nieman, M. D. Williams, R. K. Pettit, *J. Nat. Prod.* **2003**, *66*, 544. b) R. K. Pettit, B. R. Fakoury, J. C. Knight, C. A. Weber, G. R. Pettit, G. D. Cage, S. Pon, *J. Med. Microbiol.* **2004**, *53*, 61.
- [12] B. Rosenberg, L. VanCamp, J. E. Frosko, V. H. Mansour, *Nature* **1969**, *222*, 385.
- [13] R. A. Alderden, M. D. Hall, T. W. Hambley, *J. Chem. Educ.* **2006**, *83*, 728.
- [14] C. A. Rabik, M. E. Dolan, *Cancer Treat. Rev.* **2007**, *33*, 9.
- [15] W. F. Keane, L. Hart, W. W. Buchanan, *Br. J. Rheumatol.* **1997**, *36*, 560.

- [16] a) A. Kascatan-Nebioglu, M. J. Panzner, J. G. Garrison, C. A. Tessier, W. J. Youngs, *Organomet* **2004**, *23*, 1928. b) J. C. Garrison, C. A. Tessier, W. J. Youngs, *J. Organometal. Chem.* **2005**, *690*, 6008. c) L. Mercks, M. Albrecht, *Chem. Soc. Rev.* **2010**, *39*, 1903. d) L. Oehninger, R. Rubbiani, I. Ott, *Dalton Trans.* **2013**, *42*, 3269.
- [17] K. M. Hindi, M. J. Panzner, C. A. Tessier, C. L. Cannon, W. J. Youngs, *Chem. Rev.* **2009**, *109*, 3859.
- [18] a) J. C. Garrison, W. J. Youngs, *Chem. Rev.* **2005**, *105*, 3978. b) A. Kascatan-Nebioglu, M. J. Panzner, C. A. Tessier, C. L. Cannon, W. J. Youngs, *Coord. Chem. Rev.* **2007**, *251*, 884.
- [19] a) V. Milacic, D. Fregona, Q. P. Dou, *Histol. Histopathol.* **2008**, *23*, 101. b) I. Ott, *Coord. Chem. Rev.* **2009**, *253*, 1670.
- [20] D. A. Medvetz, K. M. Hindi, M. J. Panzner, A. J. Ditto, Y. H. Yun, W. J. Youngs, *Met. Based Drugs* **2008**, 384010.
- [21] R. Rubbiani, I. Kitanovic, H. Alborzina, S. Can, A. Kitanovic, L. A. Onambele, M. Stefanopoulou, Y. Geldmacher, W. S. Sheldrick, G. Wolber, A. Prokop, S. Wölfl, I. Ott, *J. Med. Chem.* **2010**, *53*, 8608.
- [22] R. A. Haque, M. A. Iqbal, S. Budagumpi, M. B. Khadeer Ahamed, A. M. S. Abdul Majid, N. Hasandudin, *Appl. Organometal. Chem.* **2013**, *27*, 214.
- [23] a) A. Moulin, S. Garcia, J. Martinez, J. A. Fehrentz, *Synthesis* **2007**, *17*, 2667. b) J. M. Crawforth, M. Paoletti, *Tetrahedron Lett.* **2009**, *50*, 4916. c) V. S. Arvapalli, G. Chen, S. Kosarev, M. E. Tan, D. Xie, L. Yet, *Tetrahedron Lett.* **2010**, *51*, 284. d) A. Zhang, X. Zheng, J. Fan, W. Shen, *Tetrahedron Lett.* **2010**, *51*, 828. e) M. Mihorianu, I. Mangalagiu, G. P. Jones, C. G. Daniliuc, M. H. Franz, I. Neda, *Rev. Roum. Chim.* **2010**, *55*, 689. f) J. T. Hutt, Z. D. Aron, *Org. Lett.* **2011**, *13*, 5256.
- [24] D. E. Kuhla, US Patent 4044015, **1997**. *Chem. Abstr.* **1977**.
- [25] a) I. Özdemir, N. Temelli, S. Günel, S. Demir, *Molecules* **2010**, *15*, 2203. b) R. Rubbiani, S. Can, I. Kitanovic, H. Alborzina, M. Stefanopoulou, M. Kokoschka, S. Mönchgesang, W. S. Sheldrick, S. Wölfl, I. Ott, *J. Med. Chem.* **2011**, *54*, 8646.
- [26] a) K. M. Hindi, T. J. Siciliano, S. Durmus, M. J. Panzner, D. A. Medvetz, D. V. Reddy, L. A. Hogue, C. E. Hovis, J. K. Hilliard, R. J. Mallet, C. A. Tessier, C. L. Cannon, W. J. Youngs, *J. Med. Chem.* **2008**, *51*, 1577. b) F. Hackenberg, G. Lally, H. Müller-Bunz, F. Paradisi, D. Quaglia, W. Streciwilk, M. Tacke, *Inorg. Chim. Acta* **2013**, *395*, 135.
- [27] T. Roth, A. M. Burger, W. A. Dengler, H. Willmann, H.-H. Fiebig, in *Relevance of Tumor Models for Anticancer Drug Development, Contributions to Oncology*, Vol. 54 (Eds: H.-H. Fiebig, A. M. Burger), Karger, Basel, **1999**, p. {0}145.
- [28] H.-H. Fiebig, W. A. Dengler, T. Roth, in *Relevance of Tumor Models for Anticancer Drug Development, Contributions to Oncology*, Vol. 54 (Eds: H.-H. Fiebig, A. M. Burger), Karger, Basel, **1999**, p. {0}29.
- [29] H.-H. Fiebig, D. P. Berger, W. A. Dengler, E. Wallbrecher, B. R. Winterhalter, *Strahlenther. Onkol.* **1992**, *42*, 321.
- [30] W. A. Dengler, J. Schulte, D. P. Berger, R. Mertelmann, H.-H. Fiebig, *Anti-Cancer Drugs* **1995**, *6*, 522.
- [31] a) J. D. Bower, G. R. Ramage, *J. Chem. Soc.* **1955**, 2834. b) W. W. Paudler, C. I. Chao Patsy, L. S. Helmick, *J. Heterocycl. Chem.* **1972**, *9*, 1157.
- [32] a) F. Firooznia, US Patent 0197582, **2007**; b) P. Blatcher, D. Middlemiss, *Tetrahedron Lett.* **1980**, *21*, 2195.
- [33] M. Alcarazo, T. Stork, A. Anoop, W. Thiel, A. Fürstner, *Angew. Chem. Int. Ed.* **2010**, *49*, 2542.
- [34] C. R. Groom, F. H. Allen, *Angew. Chem. Int. Ed.* **2014**, *53*, 662.
- [35] H. Schmidbaur, A. Schier, *Angew. Chem. Int. Ed.* **2015**, *54*, 746.
- [36] A. Kascatan-Nebioglu, A. Melaiye, K. Hindi, S. Durmus, M. J. Panzner, L. A. Hogue, R. J. Mallett, C. E. Hovis, M. Coughenour, S. D. Crosby, A. Milsted, D. L. Ely, C. A. Tessier, C. L. Cannon, W. J. Youngs, *J. Med. Chem.* **2006**, *49*, 6811.
- [37] C. V. Maftai, E. Fodor, P. G. Jones, M. Freytag, M. H. Franz, G. Kelter, H.-H. Fiebig, M. Tamm, I. Neda, *Eur. J. Med. Chem.* **2015**, *101*, 431.
- [38] A. Nandy, S. K. Dey, S. Das, R. N. Munda, J. Dinda, K. Das Saha, *Mol. Cancer* **2014**, *13*, 57.
- [39] F. Hackenberg, A. Deally, G. Lally, S. Malenke, H. Müller-Bunz, F. Paradisi, S. Patil, D. Quaglia, M. Tacke, *Int. J. Inorg. Chem.* **2012**, *2012*, 121540.

Supporting information

Additional supporting information may be found in the online version of this article at the publisher's web site.